IEEE Access
Multidisciplinary | Rapid Review | Open Access Journal

Received March 16, 2020, accepted March 25, 2020, date of publication March 30, 2020, date of current version April 16, 2020.

Digital Object Identifier 10.1109/ACCESS.2020.2983973

Design of a 3D Top-Loaded Low-Profile Sleeve Antenna for UAV Applications

LINGSHENG YANG[1], (Member, IEEE), ZILING XING[1], SHIHAO XU[1], DAN ZHANG[2], (Member, IEEE), AND YAJIE LI[3]

[1]Jiangsu Key Laboratory of Meteorological Observation and Information Processing, Research Center of Applied Electromagnetics, Nanjing University of Information Science and Technology, Nanjing 210044, China
[2]College of Information Science and Technology, Nanjing Forestry University, Nanjing 210037, China
[3]Zhongda Hospital, Southeast University, Nanjing 210009, China

Corresponding author: Yajie Li (withlove1982@163.com)

This work was supported in part by the Special Funds for Basic Scientific Research of Southeast University under Grant 2242019K40267, in part by the Priority Academic Program Development of Jiangsu Higher Education Institutions (PAPD), and in part by the Kunshan & Nanjing University of Information Science and Technology (NUIST) Intelligent Sensor Research Center Project.

ABSTRACT In this article, a 3D top-loaded low profile sleeve antenna for unmanned aerial vehicle (UAV) applications is proposed. By loading a 3D disc cone structure on the top of a sleeve antenna, the overall height of the antenna can be significantly reduced compared with the height of a traditional quarter-wavelength monopole antenna. In addition, adding shorted columns between the top plate of the disc cone and the ground can generate a new resonant point at lower frequency, so that the frequency bandwidth can be effectively extended. Finally, in order to further achieve the miniaturization of the antenna, an annular slot ring structure was etched on the upper surface of the top plate. Under the conditions of $S_{11} < -10dB$, the designed antenna with a total size of $160mm \times 160mm \times 26.6mm$ ($0.44\lambda \times 0.44\lambda \times 0.07\lambda$) has a wide band covering from 840MHz to 1.69GHz (67.2%), while the height of the proposed antenna is only 0.07λ (where λ is the wavelength of the lowest frequency point). Moreover, omnidirectional radiation performances through the operating band can be achieved for both the measured and simulated results.

INDEX TERMS Low profile, sleeve antenna, top-loaded, UAV.

I. INTRODUCTION

Recently, unmanned aerial vehicles (UAVs) have attracted lots of attentions for scientific, industrial and military applications [1]. Generally, the antenna should be compact in size to satisfy the highly limited space in UAV, light weight to prolong the endurance of the whole UAV system, and low profile to minimize air resistance for aerodynamic requirements [2]. Also in order to be robust to interference and serve multiple wireless systems simultaneously, the antenna needs to maintain well impedance matching through a wide band [3], [4]. Moreover, a monopole-like omnidirectional radiation pattern in the horizontal plane is preferable since it can enhance the communication links between the UAV and the ground base stations [5].

In order to meet the aforementioned design requirements, many research on UAV antenna designs have been reported [6]–[14]. Dielectric material loading technique was used in [6], [7]. In [6], a Co_2Z hexaferrite-glass composite was used as a helical antenna core, while in [7], conductive strip was helically wound on Co_2Z hexaferrite substrate. For both designs, antenna miniaturization can be realized, however they were not designed for wide bandwidth applications, and the radiation efficiency changes according to the dielectric performance of the material, a carefully choose is essential. In [8], double split ring resonator (DSRR) slots and vias were used to reduce the size of a planar circular patch antenna. The antenna has a 20MHz bandwidth and can cover the 1090MHz band for ADS-B (Automatic Dependant Surveillance Broadcast) applications.

In [9], the UAV antenna composes of two folded strips mounted on a ground plane. The top folded radiating strip was fed by a half-loop feeding strip. By adjusting the capacitive loads at the two ends of the radiating strip, the antenna operates in the frequency range from 500 to 511MHz, and has an omnidirectional radiation pattern. However, in order

The associate editor coordinating the review of this manuscript and approving it for publication was Giorgio Montisci.

TABLE 1. Optimized parameters (unit:mm).

Parameters	Quantity	Parameters	Quantity
r	82	r1	30
r2	5	h1	26.6
q	28.5	h2	25
q1	14.5	h3	6.5
q2	8.5	h4	18
W	0.3		

to fulfill the design goal, the ground plane should be no less than $0.5 \times 1.0m^2$ ($0.83 \times 1.67\lambda^2$), which increases the overall size of the antenna. A dual-band planar square segmented loop antenna is proposed in [10]. The loop works at the lower band around 956MHz, by using patch element and shorting strip, impedance matching at the higher band can be improved. For the two bands, the antenna was designed to have omnidirectional and quasi-omnidirectional radiation characteristics, respectively. A hemispheric conductor seamed on a $0.8 \times 0.8\lambda^2$ ground for Ultra wideband UAV applications is reported in [11]. While in [12], higher-order mode circular patch antenna operating in the frequency range of 674-719MHz was proposed. Top loaded monopole with shorting pins and inductive loading is reported in [13]. The antenna can obtain a wide bandwidth of 17% for VSWR no larger than 3. Besides these designs, monocone structures were also effective and widely used for designing low-profile, wideband antenna [14]–[16]. In [14], a 3D-printed mono-cone backed with exponentially tapered cavity is demonstrated. The antenna has a wide bandwidth and monopole-like radiation pattern. A super wide band monocone antenna is proposed in [15], by using dielectric loading, flexible impedance matching through wider bandwidth can be achieved. In [16], bent shorting strips together with parasitic and circular sleeves were used to minimize the conventional monocone antenna, a 147.3% fractional impedance bandwidth can be obtained with a low-profile.

In this paper, a 3D disc cone top-loaded sleeve antenna for UAV applications is proposed. The antenna can achieve wide band performances with a compact size and low height. Stable omnidirectional radiation patterns can be fulfilled through the whole band. The rest of the paper is organized as follows: Section II describes the design procedure of the antenna. Section III presents the measured results and discussions. Finally, conclusion is made in Section IV.

II. ANTENNA DESIGN

Figure 1 shows the geometry of the proposed antenna. The antenna comprises a sleeve antenna with a top-loaded 3D disc cone structure. The top plate of the disc cone and the ground plate are two 0.8mm thick, circular shaped FR4 substrates (relative permittivity of 4.4 and loss tangent of 0.02). Both sides of the top plate are covered with copper, while only the upper surface of the ground plate is covered with copper. The 3D structure of the cone was first made of foam, and

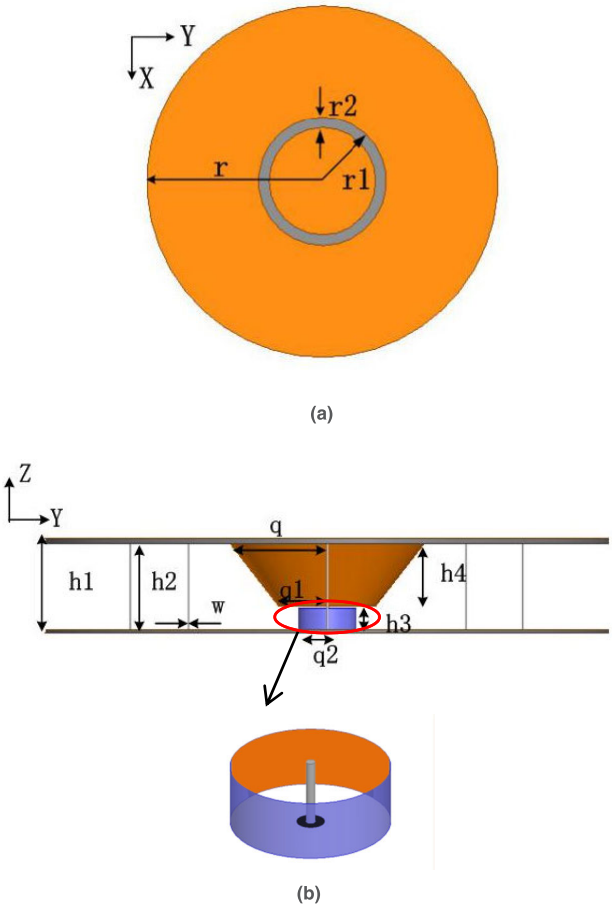

FIGURE 1. Geometrical configuration of the proposed antenna. (a) top view. (b) side view.

then the outer surface was coated with cooper. The explode-view of the feeding structure is shown in Fig.1(b), around the inner conductor of the feed, we use a cylinder shaped foam to maintain the basic shape of the sleeve, and then the outer wall of the cylinder is also coated with copper. The inner conductor is 0.5mm higher than the sleeve, so the gap between the sleeve and the cone is set as 0.5mm. Eight shorting copper columns are evenly distributed between the top plate and the ground plate according to the equal circumferential angle. The distance between the column and the feed point is 57mm. Parameters study was simulated by using ANSYS HFSS software, and the optimized parameters are listed in Table 1.

The four evolution steps to achieve the proposed antenna are shown in Fig.2. Antenna 1 is a simple sleeve antenna with a height slightly lower than $1/4\lambda$. Antenna 2 is a sleeve antenna with top-loaded 3D disc-cone structure. On the basis of antenna 2, eight shorting copper columns were added to obtain Antenna 3. Antenna 4 was designed by etching an annular slot on the upper surface of the top plate of Antenna 3.

The S_{11} curves of the four antennas are plotted in Fig.3. Antenna1 has only one resonance frequency point at around 1.5GHz. For Antenna 2, after top-loading a 3D disc-cone structure to the sleeve antenna, the resonance frequency point

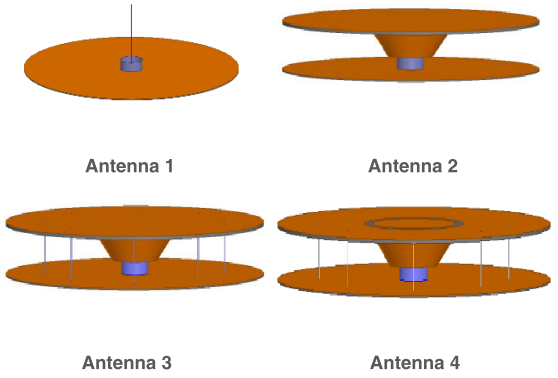

FIGURE 2. Four evolution steps of the proposed antenna.

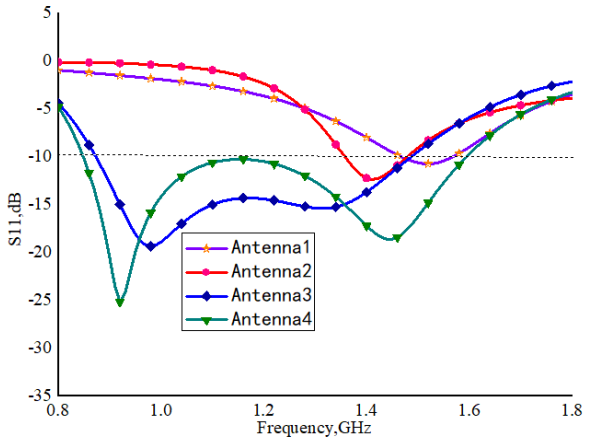

FIGURE 3. S_{11} of antenna 1, antenna 2, antenna 3 and antenna 4.

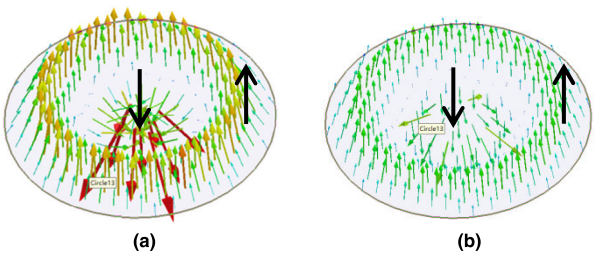

FIGURE 4. Simulated electric field of antenna 2 at two different frequencies. (a) 0.92GHz, TM02 mode. (b) 1.45GHz, TM02 mode.

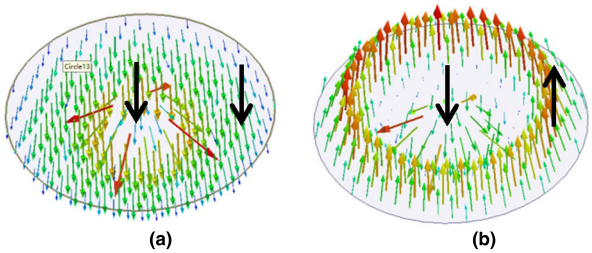

FIGURE 5. Simulated electric field of antenna 3 at two different frequencies. (a) 0.92GHz, TM01 mode. (b) 1.45GHz, TM02 mode.

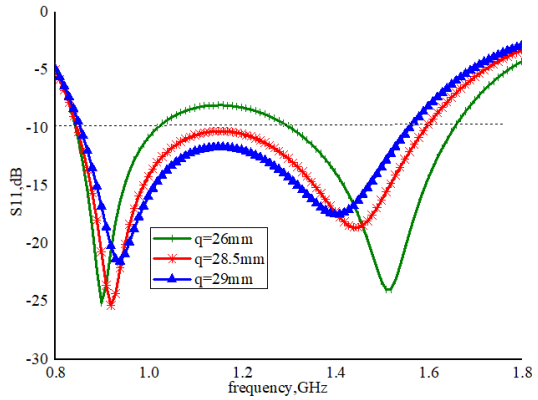

FIGURE 6. Simulated S_{11} of the proposed antenna (Antenna 4) with different q.

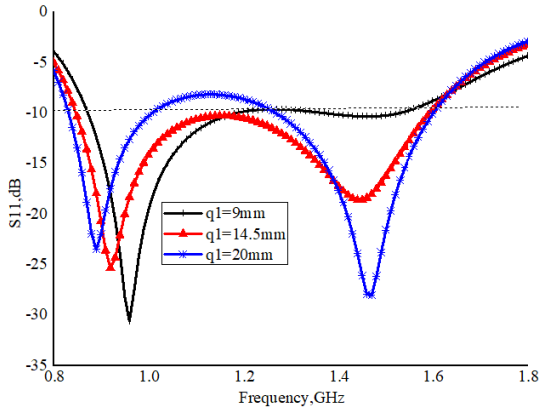

FIGURE 7. Simulated S_{11} of the proposed antenna with different q_1.

shifted to 1.4GHz, and the height of the antenna significantly reduced from $1/4\lambda$ to 0.07λ. After adding shorting columns (Antenna 3), a new resonance point was generated at the lower frequency around 0.95GHz. Compared to Antenna 3, the annular slot on the top of Antenna 4 can not only shift the resonance frequency to the lower frequency and realize antenna miniaturization, but also expand the bandwidth from 0.87-1.48GHz to 0.82-1.6GHz.

The electric field distributions between the top plate and the ground plane at 0.92GHz and 1.45GHz for antenna2 and antenna 3 (Figure 2) are illustrated in Fig.4 and Fig.5, respectively. By comparing Figure 4 and Figure 5, we can note that, at 1.45GHz, the two antennas have the same transmission mode which is the TM02 mode. While at 0.92GHz, the two antennas have different transmission modes which are TM02 mode and TM01 mode, respectively. Therefore, we concluded that the addition of the shorting columns changes the transmission mode at the lower frequency and generate a new resonance point, which is consistent with the S_{11} results shown in Figure 3.

How cone shape changes affect impedance matching are plotted in Figure 6 and Figure 7. Parameter q is the radius of the top circle of the cone. The increase of q shifts the higher resonance frequency point to lower frequency, which

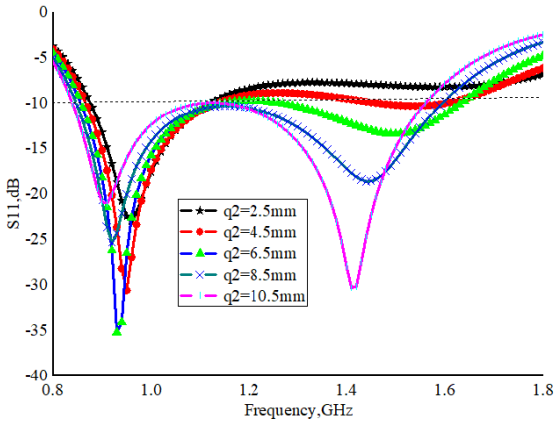

FIGURE 8. Simulated S_{11} of the proposed antenna with different q_2.

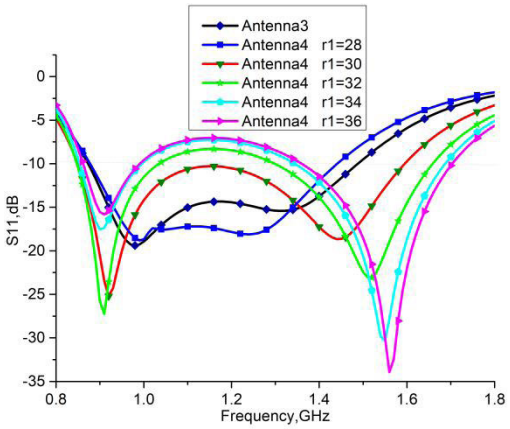

FIGURE 9. Simulated S_{11} of the proposed antenna with different r_1.

improves the impedance matching from 1.0-1.3GHz. While the radius of the bottom circle of the disc cone (q_1) mainly affects the impedance matching around the higher resonance frequency point.

Also the tilt angle of the disc cone is determined by changing the size of q and q_1. As shown in Figure 6 and Figure 7, when q equals to 28.5mm and q_1 equals to 14.5mm and the corresponding disk cone angle is 50.3°, we achieved the optimal solution.

Figure 8 shows the influence of the changes of the antenna sleeve radius (q_2) on the impedance matching. q_2 mainly affects the impedance matching around the higher resonance frequency. The larger the q_2, the better the impedance matching performance of the antenna. According to our design requirements, the q_2 is set to be 8.5mm.

Based on the aforementioned parameters studies, the mechanism of the antenna can be further explained as two one wavelength loop antennas. The frequency for the higher resonance point can be determined by the current distributed around the top circle of the cone, and the loop length is 179mm ($2\pi \times q$), which is about one wavelength at 1.45GHz. While after adding shorted columns, the distributed current length changed to the circumference which is determined by the location of the columns. Since the distance (radius) between the column and the feed point is 57mm, the circumference for the new loop on the top plate can be calculated as $2\pi \times 57 \approx 358mm$, which is about one wavelength at 0.92GHz.

The annular slot is inside the aforementioned two fed loops, and the location for the annular slot should be close to the top circle of the cone. Therefore, even if a new resonant point is generated by adding the slot, since it is close to the higher resonant frequency, the new resonant frequency point will not occur. The slot only expands the bandwidth by changing the impedance matching. As depicted in Figure 9, compared to Antenna3 (Figure 2), when the slot is inside the top circle of the cone ($r_1 < q = 28.5$mm), the slot improves the impedance matching between the two resonant frequencies, while the bandwidth becomes even narrower.

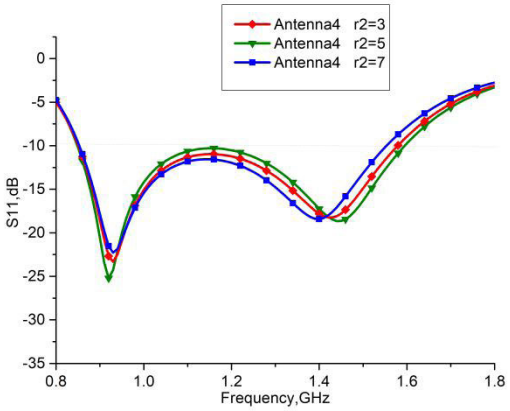

FIGURE 10. Simulated S_{11} of the proposed antenna with different r_2.

When $r_1 > q$, with the increasing of r_1, the impedance matching around the two resonant frequency points can be improved, whereas the impedance between the two resonant frequency points deteriorated. The final r_1 was set as 30mm.

As shown in Figure 10, The change of width of the slot affects the impedance matching of the antenna in some extent. While compared to the higher resonant frequency point, the width of the slot has little influences on the lower resonant frequency point.

Figure 11 depicts the simulated radiation patterns of the antenna at 0.92GHz, 1GHz, and 1.45GHz. It can be observed that through the whole operating band, the antenna has relatively stable radiation patterns. On the E-plane, the antenna has "8" shaped radiation patterns, while on the H-plane, the radiation pattern meets the requirements of the UAV antenna.

III. MEASUREMENT AND DISCUSSION

The fabricated antenna based on the optimal parameters obtained from the simulation is shown in Figure 12.

The reflection coefficients measured by the vector network analyzer is shown in Figure 13. The simulated bandwidth ranges from 0.82GHz to 1.6GHz, and

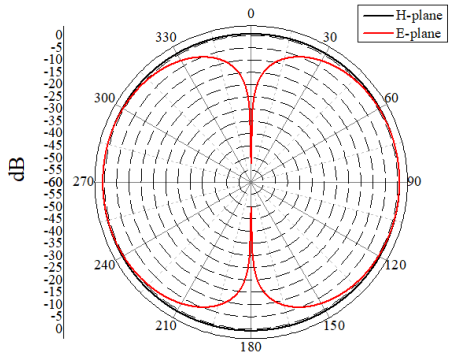

(a)

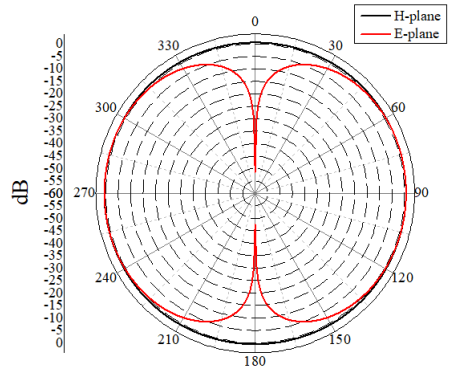

(b)

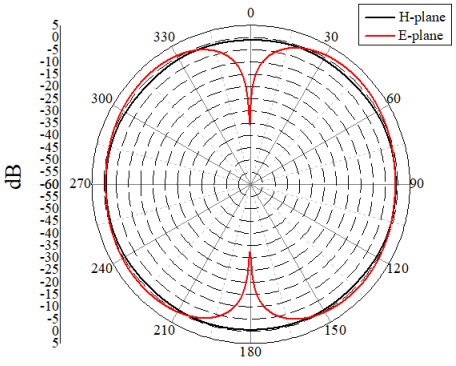

(c)

FIGURE 11. Simulated radiation patterns of the proposed antenna at (a) 0.92GHz, (b) 1GHz, (c) 1.45GHz.

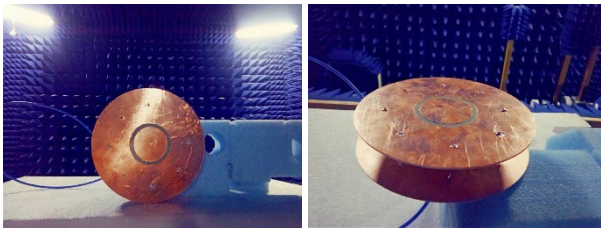

FIGURE 12. Photographs of the fabricated antenna.

the measured frequency band range is from 0.84GHz to 1.69GHz. Both results can cover the target frequency bands

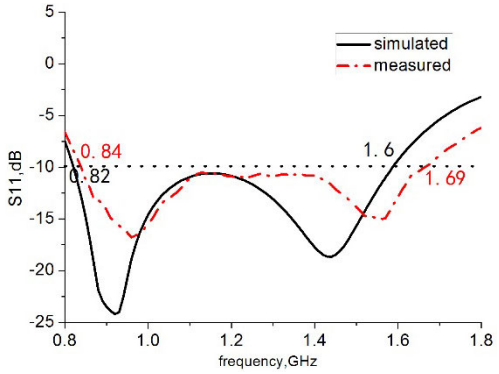

FIGURE 13. Simulated and measured S_{11}.

TABLE 2. Comparisons between the proposed and recently published UAV antenna designs.

References	Total Size (including ground/ λ^3)	Gain (dBi)	-10dB Bandwidth (%)
[8]	0.218*0.218*0.031	-0.4	11
[9]	0.27*0.083*0.05	4.8	2.2
[13]	1.39*1.39*0.03	1-4	17.3 (VSWR<3)
[11]	1.4*1.4*0.023	1.86	6.4
[15]	0.88*0.88*0.057	>3	151
Proposed	0.44*0.44*0.07	1.27-2.26	67.2

like ADS-B (978MHz/1090MHz), GSM850/900, L-band (0.96-1.22GHz) and so on, but compared with the simulation results, the measured results are shifted to higher frequency because of the manufacturing errors and the differences between the actual material and the ideal model in the simulation.

We measured the fabricated antenna in the anechoic chamber. Figure 14(a) and (b) depict the simulated and measured radiation patterns of the proposed antenna in the H-plane and E-plane separately at the central frequency of 1 GHz. We can observe that the measured and simulated results are in good agreement. In E-plane, the max radiation occurs at 220 degree. While the fluctuation is smaller than 1dB in H-plane, which indicates that a measured omnidirectional radiation property of the proposed antenna is obtained.

Figure 15 presents the simulated and measured peak gain of the proposed antenna. The simulated peak gain varies from 1.31-2.21dBi and the measured peak gain varies from 1.27 to 2.26dBi. Meanwhile, through the operating band, the simulated radiation efficiency is higher than 92%, which also proves the good performance of the antenna.

For UAV applications, the antenna design needs to consider the height, footprint, bandwidth, gain and other factors. The comparisons between the proposed antenna and the UAV antenna research results published in recent years are listed in Table 2. It can be seen that the proposed antenna is relatively small in size and low in height, simultaneously, it has a wide band and acceptable radiation perfor-

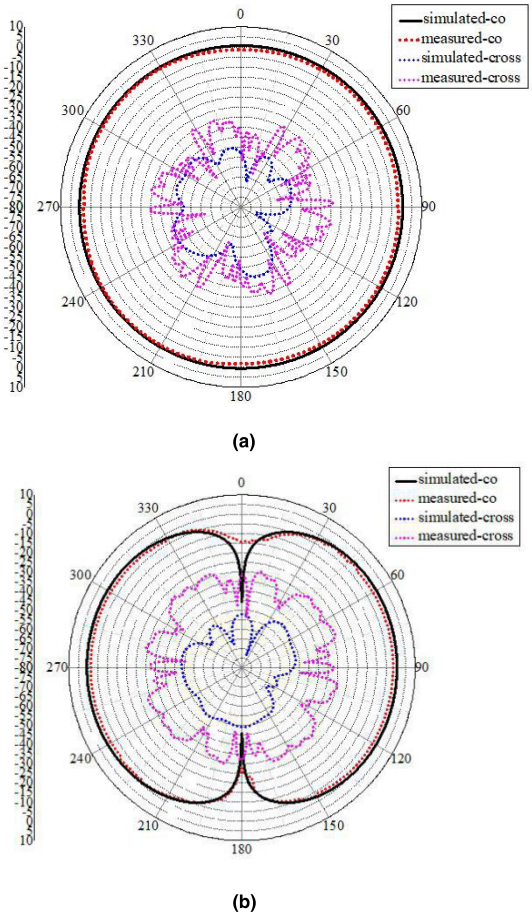

FIGURE 14. Simulated and measured radiation patterns of the proposed antenna in the (a) H-plane and (b) E-plane at 1 GHz.

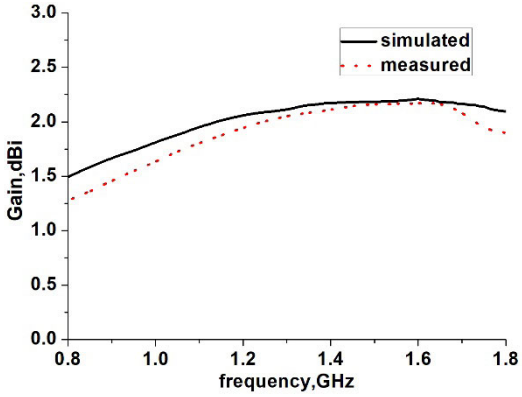

FIGURE 15. Simulated and measured peak gain of the proposed antenna.

mances. Also, the performances of the proposed antenna was evaluated with a much smaller ground (the size of the ground is the same as the top plate), when the antenna was mounted on the UAV, better radiation performances can be expected.

IV. CONCLUSION

In this article, a top-loaded sleeve antenna for UAV applications was proposed. We loaded a 3D disc cone to reduce the height of the antenna, added eight shorted columns to achieve lower frequency resonance and utilized the annular slot structure to further increase the bandwidth of the antenna. Finally, the fabricated antenna can achieve coverage in the 0.84-1.69GHz band under the condition of the miniaturization at low profile. The proposed antenna can obtain an omnidirectional property in the frequency band with stable radiation characteristics, which meets the performance requirements of UAV applications.

REFERENCES

[1] B. T. Strojny and R. G. Rojas, "Bifilar helix GNSS antenna for unmanned aerial vehicle applications," *IEEE Antennas Wireless Propag. Lett.*, vol. 13, pp. 1164–1167, 2014.

[2] L. Scorrano, A. Di Rosa, B. Orobello, A. Manna, and F. Trotta, "Experimental investigations of a novel lightweight blade antenna for UAV applications [antenna applications Corner]," *IEEE Antennas Propag. Mag.*, vol. 59, no. 2, pp. 108–178, Apr. 2017, doi: 10.1109/MAP.2017.2655533.

[3] D. Wu, X. Chen, L. Yang, G. Fu, and X. Shi, "Compact and low-profile omnidirectional circularly polarized antenna with four coupling arcs for UAV applications," *IEEE Antennas Wireless Propag. Lett.*, vol. 16, pp. 2919–2922, 2017, doi: 10.1109/LAWP.2017.2752358.

[4] Z.-Q. Liu, Y.-S. Zhang, Z. Qian, Z. P. Han, and W. Ni, "A novel broad beamwidth conformal antenna on unmanned aerial vehicle," *IEEE Antennas Wireless Propag. Lett.*, vol. 11, pp. 196–199, 2012.

[5] M. Nosrati, A. Jafargholi, R. Pazoki, and N. Tavassolian, "Broadband slotted blade dipole antenna for airborne UAV applications," *IEEE Trans. Antennas Propag.*, vol. 66, no. 8, pp. 3857–3864, Aug. 2018, doi: 10.1109/TAP.2018.2835524.

[6] N. Neveu, Y.-K. Hong, J. Lee, J. Park, G. Abo, W. Lee, and D. Gillespie, "Miniature hexaferrite axial-mode helical antenna for unmanned aerial vehicle applications," *IEEE Trans. Magn.*, vol. 49, no. 7, pp. 4265–4268, Jul. 2013.

[7] W. Lee, Y. K. Hong, J. Lee, D. Gillespie, K. G. Ricks, F. Hu, and J. Abu-Qahouq, "Dual-polarized hexaferrite antenna for unmanned aerial vehicle applications," *IEEE Antennas Wireless Propag. Lett.*, vol. 12, pp. 765–768, 2013.

[8] S. Yan, S. S. Wang, Y. Hu, and A. E. Vandenbosch, "Low-profile omnidirectional antenna for automatic dependent surveillance—Broadcast applications," *Electron. Lett.*, vol. 51, no. 22, pp. 1732–1734, Oct. 2015.

[9] B.-H. Sun, Y.-F. Wei, S.-G. Zhou, and Q.-Z. Liu, "Low-profile and horizontally-polarised antenna for UAV applications," *Electron. Lett.*, vol. 45, no. 22, pp. 1106–1107, 2009.

[10] D. Kang, J. Tak, and J. Choi, "Wideband low-profile planar square segmented loop antenna for UAV applications," *Electron. Lett.*, vol. 52, no. 22, pp. 1828–1830, Oct. 2016.

[11] J.-Y. Jeong and J.-M. Woo, "Ultra-wide band antenna attachable on UAV surface," *Int. J. RF Microw. Comput.-Aided Eng.*, vol. 27, no. 8, Oct. 2017, Art. no. e21129.

[12] J. Tak and J. Choi, "A flush-mounted monopolar patch antenna for UAV applications," *Microw. Opt. Technol. Lett.*, vol. 59, no. 5, pp. 1202–1207, May 2017.

[13] L. Akhoondzadeh-Asl, J. Hill, J.-J. Laurin, and M. Riel, "Novel low profile wideband monopole antenna for avionics applications," *IEEE Trans. Antennas Propag.*, vol. 61, no. 11, pp. 5766–5770, Nov. 2013.

[14] S. Lee, G. Jeoung, and J. Choi, "Three-dimensional-printed tapered cavity-backed flush-mountable wideband antenna for UAV," *Microw. Opt. Technol. Lett.*, vol. 59, no. 12, pp. 2975–2981, Dec. 2017.

[15] A. Liu and Y. Lu, "A superwide bandwidth low-profile monocone antenna with dielectric loading," *IEEE Trans. Antennas Propag.*, vol. 67, no. 6, pp. 4173–4177, Jun. 2019.

[16] K.-S. Keum, Y.-M. Park, and J.-H. Choi, "A low-profile wideband monocone antenna using bent shorting strips," *Appl. Sci.*, vol. 9, no. 9, p. 1896, 2019.

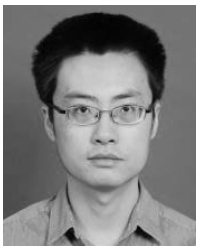

LINGSHENG YANG (Member, IEEE) received the B.S. degree from the Department of Communication Engineering, Nanjing University of Science and Technology, China, in 2001, and the M.S. and Ph.D. degrees from the Faculty of Information Science and Electrical Engineering, Kyushu University, Japan, in 2009 and 2012, respectively.

Since 2012, he has been an Assistant Professor with the Electronics and Information Engineering Department, Nanjing University of Information Science and Technology. He is the author of more than 40 articles and more than 30 inventions. His research interests include antenna theory and design, MIMO, EMC, bioelectromagnetics, and lightning detection.

ZILING XING was born in Nanjing, Jiangsu, China, in 1999. She is currently pursuing the bachelor's degree with the Electronics and Information Engineering Department, Nanjing University of Information Science and Technology. Her research interests include antennas and signal processing.

SHIHAO XU was born in Suqian, Jiangsu, China, in 1994. He received the bachelor's degree in communications engineering from the Nanjing Institute of Technology, in 2018. He is currently pursuing the degree with the Department of Electronics and Information Engineering, Nanjing University of Information Science and Technology. His research interest includes antennas and electromagnetic energy transformation.

DAN ZHANG (Member, IEEE) received the B.S. degree in mechanical engineering from the Dalian University of Technology, Dalian, China, in 1999, and the M.S. and Ph.D. degrees in electromagnetic waves and communication engineering from Kyushu University, Fukuoka, Japan, in 2004 and 2007, respectively. In 2015, he was introduced with Nanjing Forestry University, China, as a high-level talent. He is currently a Professor of electronic and communication engineering with the College of Information Science and Technology, Nanjing Forestry University. In recent years, more than 50 articles have been published by the first author and more than ten patents have been applied for granted. His research interests include electromagnetic field theory, microwave and optical technology, and nondestructive testing and imaging. He has been invited by the International Professional Society for many times to preside over international conferences or give academic speeches. He is also an Associate Editor of *IEICE Electronics Express* and a Reviewer of several internationally renowned professional journals.

YAJIE LI received the B.S. and M.S. degrees from the School of Medicine, Zhejiang University, China, in 2005 and 2007, respectively.

From 2007 to 2012, she worked with The First Affiliated Hospital, Wenzhou Medical University. Since 2012, she has been an Attending Doctor with the Geriatric Department, Zhongda Hospital, Southeast University. She is the author of nearly 20 articles. Her research interests include gerontology, internal medicine of digesting, medical engineering, and bioelectromagnetics.